CO_2 Capture by ion exchange resins as amine functionalised adsorbents

CO_2 Capture by ion exchange resins as amine functionalised adsorbents

Mahmoud Parvazinia, Susana Garcia, Mercedes Maroto-Valer

PII: S1385-8947(17)31431-6
DOI: http://dx.doi.org/10.1016/j.cej.2017.08.087
Reference: CEJ 17538

To appear in: *Chemical Engineering Journal*

Received Date: 8 June 2017
Revised Date: 16 August 2017
Accepted Date: 17 August 2017

Please cite this article as: M. Parvazinia, S. Garcia, M. Maroto-Valer, CO_2 Capture by ion exchange resins as amine functionalised adsorbents, *Chemical Engineering Journal* (2017), doi: http://dx.doi.org/10.1016/j.cej.2017.08.087

CO_2 Capture by ion exchange resins as amine functionalised adsorbents

Mahmoud Parvazinia[a,b], Susana Garcia[a], Mercedes Maroto-Valer[a]

[a] Centre for Innovation in Carbon Capture and Storage (CICCS), School of Engineering & Physical Sciences, Heriot-Watt University, Edinburgh, UK

[b] Iran Polymer and Petrochemical Institute, Tehran, Iran

Abstract:

In this work, the performance of ion exchange resins as amine functionalised CO_2 adsorbents is evaluated. These resins are D201 and D202 of Jiangsu Suqing Water Treatment Engineering Group Co.,Ltd, Purolite A109, A830 and Lewatit VPOC1065. A109 and VPOC1065 show higher CO_2 adsorption performance than D201, D202 and A830. VPOC1065 and A109 are functionalised with primary amines on a polymeric support of styrene cross-linked with divinylbenzene. Their capture capacity is examined at different temperatures, ranging from 25 to 80^{o}C, and different CO_2/N_2 ratios (0.02 to 0.98) in a dry gas mixture, using thermogravimetric analysis. VPOC1065 and A109 show a capacity of 1.75 and 1.12 mmol/g at 25^{o}C and 98% CO_2/N_2, respectively. Complete regeneration at 105^{o}C can be achieved for both resins and they exhibit fast adsorption and desorption kinetics. Cyclic adsorption-desorption tests are also performed and VPOC1065 shows excellent stability in 275 cycles. Hence, VPOC1065 and A109 ion exchange resins proved to be promising candidates for CO_2 adsorption.

Key Words: CO_2, Adsorption, Cyclic stability, Amine, Polymer, Ion exchange resin

1. Introduction:

The main source of energy for the coming decades seems to be fossil fuels [1]. Fossil fuels emit CO_2 in the atmosphere, which contributes to the greenhouse effect and climate change. For sustainable use of fossil fuels, CO_2 emission management is of vital importance. Fossil fuel-fired power plants are one of the major sources of CO_2 emissions [2]. The separation of CO_2 from other gases has been clearly conducted for a few decades in the natural gas industry as usually reservoirs contains some amounts of CO_2 [3]. Commercial CO_2 capture processes are based on using alkanolamine solvents such as monoethanolamine (MEA) but the main drawbacks of these liquid amine-based processes are their high regeneration energy, solvent degradation, equipment corrosion and scale up problems [4].

Porous solid adsorbents with low heat capacities represent an interesting alternative to amine aqueous systems for CO_2 capture, due to their higher gas phase mass diffusion into the porous support and elimination of corrosion of process equipment. However, CO_2 adsorption by porous solid adsorbents still needs more work, which is mainly focused on optimizing adsorption performance by developing appropriate materials [5,6]. Most widely used porous solid materials are silica, alumina, zeolite, carbon and more recently polymeric and MOF materials. The amine groups can be immobilised on porous support solids in favour of chemisorption that enhances capacity and selectivity in comparison with physisorption [7,8]. For adsorbents to be competitive with aqueous amine solutions, a stable capacity of about 3 mmol CO_2/g ads is desirable in flue gas

conditions [9]. Many works have been done on CO_2 adsorption but more research is needed in order to develop solid adsorbents with optimum performance for CO_2 adsorption [6, 9- 11].

Impregnation techniques have been widely used to functionalise porous support materials. Although the impregnation technique increases adsorption capacity due to high level of amine loading but, possible amine leaching into the gas phase reduces cyclic adsorption-desorption stability [12-15]. To overcome amine leaching (amine evaporation) it is possible to immobilise the amine by covalent bonding with the porous solid support [16]. But the amine loading is limited to the functional groups in the support [10, 17-21].

Porous polymeric materials have been used as porous solid support for functionalization with amines. Impregnation method was used in a number of works for amine functionalisation of polymethylmethacrylate (PMMA) as porous polymer support [22-26]. More works have been done with porous polymers with N functionality for CO2 capture as support materials [27-34]. Chitsiga et al [35] applied poly-succinimide (PSI) as support and covalent bonding using grafting technique with water-soluble amines to study CO_2 capture.

A class of polymeric materials that are generally used for water treatment are ion exchange resins (IERs). They are crosslinked polymers normally based on acrylic or styrene monomers. These polymers are functionalised with amines as anion exchanger in water treatment. For water treatment, they are mainly functionalised with quaternary amines to preserve exchange capacity in a wide range of pH. Other amines are used for some special purpose cases. The macroporous anion exchangers can be regarded as potential candidates for CO_2 capture as amine functionalised adsorbents. A few studies have been done on IERs using Lewatit VPOC1065 that is functionalized with primary amine. Alesi and kitchin [16] evaluated the CO_2 capture capacity of commercial Lewatit VPOC1065 anion exchange resins. They reported a CO_2 capture capacity of 2.5 mmolCO_2/g ads at 50^{o}C and dry gas conditions for 100% CO_2 using Cahn TG-131 thermogravimetric analyzer (TGA). By exposing the resin to a dry gas mixture of 10% CO_2 in N_2, the adsorption capacity is about 1.55 mmolCO_2/g ads in a fixed bed reactor. Eighteen cycles of temperature swing regeneration were done with 10% CO_2 in N_2 gas mixture and adsorption temperature of 50^{o}C and desorption of 120^{o}C. They observed no apparent reduction in adsorption capacity. These resins shipped wet containing about 50% water. The resin was dried at 110^{o}C for 3 hr in N_2 to remove moisture before performing adsorption experiments. Veneman et al. [36] also examined the Lewatit VPOC1065 materials for post combustion CO_2 capture. The highest CO_2 capture measured was 2.8 mmol CO_2/g ads at 30^{o}C, 70 kpa pressure in 80 vol% of CO_2 gas mixture, dry condition using NETSZCH STA 449 F1 Jupiter thermal gravimetric analyzer (TGA). By increasing the temperature, capture capacity decreased. They examined the H_2O uptake in humid gas conditions. Their results showed the CO_2 uptake is not affected by the co-adsorption of H_2O. The sample was heated up to 80^{o}C in N_2 to desorb any pre-adsorbed CO_2 and moisture. Hallenbeck et al. [37] investigated the stability of VPOC1065 in the presence of O_2 and SO_2. The degradation against O_2 was examined by 17 cycles of adsorption/desorption via a thermal swing between 50 and 127^{o}C and using a test gas of 12 vol % CO_2, 4% O_2, 84% N_2 in a fixed bed reactor. A stable cyclic adsorption-desorption capacity of about 1.27 mmol CO_2/g ads was reported. A test gas of 12.5 vol % CO_2, 4% O_2, 431 ppm SO_2, and balance N_2 was used to evaluate the stability against SO_2 over the same number of cycles. After 12

cycles the capture capacity linearly reduces to about 0.2 mmol CO_2/g ads (from the average of 1.27 mmol CO_2/g ads).

In this work a few available anion exchange resins are examined to evaluate existing commercial resins. These resins are developed for water treatment and therefore not necessarily optimized for CO_2 capture. Lewatit VPOC1065 and Purolite A109 are both functionalised with primary amines. Most ion exchange resins are functionalised with quaternary amines for water treatment. D201 and D202 of Jiangsu Suqing Water Treatment Engineering Group Co.,Ltd A830 are also evaluated for CO_2 adsorption using a dry gas mixture of CO_2 in N_2. D201 and D202 are functionalised with quaternary amine and A830 with complex amine based on the manufacturer data sheet. The study is focused on A109 and VPOC 1065. The resins were dried in a tube directly from wet under N_2 and 110^{o}C for 50 hr to be sure that there is no moisture in the core of the beads. Another issue with these resins is their shrinkage in the absence of moisture [16]. Since our experiments are performed in dry conditions, 50 hr of drying was used to be sure about structural stability and no extra shrinkage in the course of experiments particularly cyclic adsorption-desorption tests. CO_2 adsorption in a temperature range of 25-80°C and CO_2/N_2 ratio of 0.02-0.98 is investigated. Different desorption temperatures under pure N_2 were studied to evaluate complete desorption. Cyclic adsorption-desorption tests to study the stability and duration of the adsorbents are performed.

2. Methodology

2.1. Resin samples

Five different commercial macroporous ion exchange resins are evaluated in this work including D201 and D202 of Jiangsu Suqing Water Treatment Engineering Group Co. Ltd., Purolite A109 and A830 and Lewatit VPOC1065. A summary of manufacturer data is shown in Table 1.

Table1. Manufacturer data on the commercial ion exchange resins used in this work

Ion exchange resins	Amine group	Ion exchange capacity	Particle size mm	moisture	Support materials
VPOC 1065	Primary amine	2.2 eq/lit	0.315-1.25	65-70%	Polystyrene-divinylbenzene
A109	Primary amine	1eq/lit	0.425-1	58-65%	Polystyrene-divinylbenzene
D201	quaternary amine	0.95-1.2 mmol/ml (3.7 mmol/g)	0.315 -1.25	50-60%	Polystyrene-divinylbenzene
D202	quaternary amine	3.6 mmol/g	0.315-1.25	47-57%	Polystyrene-divinylbenzene
A830	complex amine	2.75 eq/lit	0.3-1.2	50-56%	polyacrilic-Divinylbenzene

For Lewatite VPOC1065 textural properties are reported by manufacturer as: BET surface area of 50m^2/g, pore volume of 0.27cm^3/g and pore size of 25nm. For other samples manufacturer has not provided any textural data. The chemical formula of amine groups are not reported by manufacturer.

2.2 Samples Characterization:

A Micromeritics Gemini VII 2390 Surface Area Analyser is used to measure surface area and pore volume, and the results are shown in Table 2. For BET surface area, a low-pressure region of 13 points from 0.01 to 0.25 relative pressures is used. One point pore volume at a relative pressure of 0.984 is reported in Table 2.

Table2. Textural properties of the samples after 50 hr drying at 110^{o}C under N_2

Ion exchange resins	BET surface area m^2/g	Pore volume cm^3/g
VPOC1065	24.5811	0.202653
A109	25.5314	0.033331
D201	9.0443	0.015320
D202	7.1163	0.013251
A830	4.4135	0.009138

FTIR experiment is performed using PerkinElmer instrument. CHN elemental analysis is done using CEC-440 Elemental Analyser.

Table3. CHN elemental analysis of samples A109 and VPOC1065

	C%	H%	N%
VPOC1065	80.85	7.91	8.86
A109	81.28	7.37	6.13

Table 3 shows CHN elemental analysis. The instrument is a CEC-440 Elemental Analyzer. The carrier gas is CP grade helium, the sample is weighed (~1.7 mg) into a tin capsule and sealed. Followed by combustion for 60 seconds with oxygen at 975^{o}C, the resultant gases are converted to CO_2, H_2O and N_2 via series of chemicals and detected by a thermal conductivity detector. The support for VPOC1065 and A109 is polystyrene-divinylbenzene that the divinylbenzene content is not necessarily same. C and H content are reasonably similar but N content of A109 is clearly lower than VPOC1065 that shows lower amine loading. CHN elemental analysis is just performed for A109 and VPOC1065 as the current work focuses on these two samples.

The CO_2 capture performance of IERs is determined by using thermal gravimetric analyser (TGA) (TA instruments Q500). The sample is first heated up to 120^{o}C for 30 min for desorption of H_2O traces and other possible adsorbed molecules. Then the temperature is reduced to adsorption temperature and after equilibration, CO_2 is then introduced at the selected concentration in the gas mixture to measure CO_2 adsorption capacity of the resin samples. In the cyclic adsorption-desorption tests, first adsorption of CO_2 performs for 20 min under 10% CO_2/N_2 at 50°C which is followed by desorption under N_2 at 105^{o}C for 10min. All experiments are performed at a total flow rate of 50mL/min for dry gas mixture.

3. Results and discussions

In this work, the CO_2 capture capacity of the resin samples is studied from 25 to 80^oC and five different CO_2/N_2 ratios (from 0.02 to 0.98), as well as their adsorption and desorption rates and cyclic adsorption-desorption stability by using the thermal gravimetric analyser (TGA).

Drying of the samples has strong effect on textural properties and capture capacity. As Table 1 shows, they are shipped wet and drying is needed prior to experiments. These ion exchange resins swell in water. Alesi and Kitchin [16] have also shown that drying reduces the surface area and particularly pore volume. Table 4 shows the effect of drying time span on textural properties of VPOC1065 and A109. In this work, all samples are dried for 50 hr at 110^oC under N_2 in tube with L/D=10 directly from wet to remove all water content. Alesi and Kitchin [16] worked in humid gas conditions and dried the resins for 3 hr at 110^oC under N_2. As it can be seen from Table 4, the changes in surface area are minor for VPOC1065 while for A109 there is a considerable reduction when drying increases to 50 hr. For both samples, pore volume reduces about 50% as drying time increases from 4 to 96hrs. The reason for reduction in the surface area and pore volume can be referred to support polymeric structure. This is also pointed out by Alesi and Kitchin [16]. The three dimensional cross linked polymeric support shows shrinkage as it gets dried. A109 shows more shrinkage than VPOC1065 possibly because of less crosslinking density of A109 (possibly less divinylbenzene is applied as cross-linker). The shrinkage of the support has been mentioned by Alesi and Kitchin [16]. They have mentioned that extensive drying of the resin shrinks the resin and reducing the capacity. Since this work is done under dry conditions therefore, extensive drying to reach stability is applied although the capacity is reduced.

Table4. Effect of drying time on textural properties of VPOC1065 and A109 at 110^oC under N_2

	Drying time span hrs	BET surface area m^2/g	Pore volume cm^3/g
VPOC1065	4	25.1646	0.218269
VPOC1065	50	24.5811	0.202653
VPOC1065	96	22.6692	0.120896
A109	4	45.6556	0.057581
A109	50	25.5314	0.033331
A109	96	26.5231	0.025725

3.1 CO_2 Capture capacity

Fig. 1 shows the TGA results for five available commercial grade ion exchange resins. Due to quaternary amine groups, D201 and D202 show lower CO_2 adsorption capacity together with low rate of adsorption. Table 2 shows that the surface area and pore volume of D201, D202 and A830 are lower than VPOC1065 and A109 that can be regarded as the reason for lower CO_2 capture capacity and slow rate of adsorption.

CO_2 capture capacity for A109 and VPOC1065 are examined at different temperatures (25, 35, 50, 65 and 80°C) and CO_2/N_2 rations (0.02, 0.1, 0.4, 0.7 and 0.98, see Fig. 2a and 2b) to study CO_2 capture performance. Figs. 2a and 2b indicate that the capture capacity of VPOC1065 is much higher than the A109. The higher capture capacity of VPOC1065 can be explained by higher amine loading as indicated in Table 3 and higher pore volume of VPOC1065 as reported in Table 2. Beside it, although both resins are functionalised with primary amine groups but they are not necessarily same amine molecules and this difference can be responsible for lower capture capacity of A109. As Table 1 shows, the ion exchange capacity of VPOC1065 is 2.2 times higher than that for A109 but CO_2 capture capacity for VPOC1065 at 25°C and 98% CO_2 is 1.7 times higher than that for A109. This shows that all available amine sites for ion exchange in water are not accessible for CO_2. The gaseous CO_2 has access to the surface amine groups while in water treatment, the diffusion of water in the bulk of swelled polymer make the bulk amine groups accessible, providing higher capacity than for CO_2 adsorption.

As Figs. 2a and 2b show, by increasing the temperature, capture capacity decreases at all CO_2/N_2 ratios. This observation is in agreement with what is usually expected for simple amine molecules that shows no diffusion resistance [21,38]. As the CO_2 adsorption is exothermic therefore, by increasing the temperature desorption favours although the diffusion of CO_2 increases by increasing temperature [38]. By increasing the CO_2 concentration in feed gas, the capacity increases accordingly for both VPOC1065 and A109. Therefore in this work, it is assumed that the system is not diffusion (kinetic) controlled and heat of adsorption reduces the capacity by increasing the temperature, which means that the system is thermodynamic controlled [21].

There is a meaningful difference in the reduction and increase of capacities of A109 and VPOC1065. Fig. 2a shows that by increasing the temperature from 25 to 80°C under 0.98 CO_2/N_2, VPOC1065 capacity reduces from 1.748 to 1.198 mmol CO_2/g ads, i.e. 31.46% reduction. For A109 the capacity reduces from 1.123 to 0.373 mmol CO_2/g ads (66.76% reduction), i.e., about twice more than VPOC1065. This shows that the bonding between CO_2 and amine functional groups in VPOC1065 is stronger than that in A109. When the CO_2 concentration is reduced from 0.98 to 0.02, VPOC1065 shows less reduction in capture capacity. This can be related to higher amine loading and therefore more accessible benzyl-amine active sites in VPOC1065 and partly it can be seen as a reason for stronger interaction between CO_2 and amine group in VPOC1065.

Theoretical capacity of VPOC1065 can be calculated using the molecular weight of the free base resin. If we suppose that 10% cross linker (divinylbenzene) has been used in the resin that cannot bond with amine group then a maximum of 6.75 mmol N/g ads can be loaded. Alesi and Kitchin [16] has also calculated this theoretical capacity. In dry gas mixture each two N bond with one CO_2 molecule and therefore maximum capacity would be 3.375 mmol CO_2/g ads.

The capture capacity of amine-functionalised adsorbents strongly depends on the functionalization method. With impregnation as the amine loading is higher, the capture capacity is higher too. For example TEPA (Tetraethylenepentamine) impregnated MCM41 shows a capacity of 5.45 mmol CO_2/g ads at 75°C under pure CO2 [39] and APS (aminopropylsilane) grafted MCM41 shows a capacity of 0.64 mmol CO_2/g ads at 50°C under

pure CO_2 [38]. The statistics show that samples with grafting usually produce a capacity of less than 2 mmol CO_2/g ads [40, 41, 42]. The reason is limited silanol groups in silica materials. Here for ion exchange resins also there is limited amount of benzene molecules to form benzyl-amine active sites. In the case of ion exchange resins, as it was discussed, seems more amine loading with respect to theoretical capacity is possible.

3.2 CO_2 adsorption dynamic

The rate of CO_2 adsorption graphs is obtained from CO_2 adsorption data using TGA. As Figs. 3 and 4 show, by increasing the temperature and decreasing the CO_2 concentration in the feed gas mixture, the rate of adsorption decreases for VPOC1065 and A109. VPOC1065 shows higher adsorption rate than A109, possibly due to more amine loading and therefore, higher density of benzyl-amine active sites. When the adsorption temperature is increased at a fix CO_2 concentration, the maximum rate of adsorption is observed at same moment (see Figs, 4a and 4b). However, by decreasing the CO_2 concentration from 0.98 to 0.02 CO_2/N_2 at a fix temperature, the maximum adsorption rate is observed later accordingly (see Figs 3a and 3b). This is possibly a reason for lower diffusion rate of CO_2 inside the porous body of adsorbent when the CO_2 concentration decreases in the gas mixture of CO_2 in N_2.

Meth et al [43] have reported three different regions in CO_2 adsorption, namely, initial, intermediate and final adsorption regions. High adsorption rate corresponds to the initial adsorption region, which is followed by a transition region known as intermediate, and finally the flat region with low to zero adsorption rate, which is referred to final adsorption region. Here, with respect to adsorption rate graphs in Figs. 3 and 4 at initial region, a sharp rise can be seen in adsorption rate in the first few minutes, then the adsorption rate decreases and finally there is a flat zone in which we have no or low CO_2 adsorption. To quantify the dynamic behaviour of CO_2 adsorption, the 2nd derivative of CO_2 adsorption data, i.e., CO_2 adsorption acceleration is shown in Figs. 5a and 5b. These curves are shown at 98% CO_2/N_2 and at 25 and 80^{o}C for both VPOC1065 and A109. By using this plot, three regions can be clearly distinguished based on CO_2 adsorption acceleration. The first region of high adsorption rate shows a positive peak, the transition region shows a negative peak and the third region is a flat curve with zero acceleration (it does not mean zero adsorption). At 25^{o}C VPOC1065 shows a peak of about 2.5 while for A109 it is less than mmol CO_2/g ads.min^2. The 2nd peak shows about -1.1 mmol CO_2/g ads.min^2 for both samples and then after less than 3 minutes it is zero that shows a constant rate of adsorption. Hence, both samples have a similar dynamic behaviour in the transition zone, which seems mainly to be a shift from chemisorption to physisorption. In other words, the rate of adsorption for VPOC1065 and A109 reduces with same dynamic in transition zone. In the first region chemisorption is dominant with high rate of adsorption and positive CO_2 adsorption acceleration. The 2nd region can be interpreted as a transition zone between chemisorption and physisorption mechanisms, with negative CO_2 adsorption acceleration. In the third region, CO_2 molecules have mostly occupied the amine active sites and therefore physisorption is dominant, rate of adsorption is low and constant and CO_2 adsorption acceleration is zero.

3.3 Desorption conditions

CO_2 desorption conditions are very important in determining the required energy consumption for regeneration of adsorbent. Energy consumption is an important issue for a commercial CO_2 adsorbent. Here for CO_2 desorption temperature swing (TSA) is applied using pure N_2. Desorption at relatively low temperature with fast desorption rate is desirable. Before running the cyclic adsorption-desorption experiments, the desorption temperature under pure N_2 were determined. Figs. 6a and 6b show the results for desorption of VPOC1065 and A109. Three different desorption temperatures 90, 105 and 120^{o}C were evaluated. As Figs. 6a and 6b show, desorption at 105^{o}C is quite similar to 120°C that shows complete desorption and therefore desorption were performed at 105^{o}C. A109 shows complete and similar desorption at all three desorption temperatures. As Fig. 6a shows, at 90^{o}C CO_2 desorption for VPOC1065 is slower in comparison with two other desorption temperatures. It shows that the bonding between amine group and CO_2 in A109 is weaker than VPOC1065. This was seen earlier in section 3.1 when by increasing the temperature, VPOC1065 showed less reduction in capture capacity.

3.4 Cyclic adsorption-desorption tests

Cyclic adsorption-desorption tests were performed for both samples of A109 and VPOC1065. Cyclic stability and durability is an important practical parameter to make an adsorbent applicable. Figs. 7a and 7b show the results for cyclic adsorption-desorption tests. The desorption temperature and time is selected based on desorption tests mentioned in section 3.3 (see also Figs. 6a and 6b). This adsorption-desorption cycles were performed for both samples of VPOC1065 and A109. While after 40 cycles VPOC1065 shows just about 1.42% reduction in capacity, A109 shows about 11.24%. In a test of 275 adsorption-desorption cycles, VOPC1065 shows just 4.84 % reduction in capacity. As Fig 6b illustrates, A109 shows complete desorption at 90 similar to 105 and 120^{o}C. Cyclic stability at desorption temperature of 90^{o}C is shown in Fig. 7c for A109 but there is still 10.65% reduction in capture capacity. 15^{o}C reduction in desorption temperature did not improve the stability of A109.

To study the reason for CO_2 capture capacity reduction, FTIR test was performed. It is generally accepted that the reason for reduction in capacity during cyclic adsorption-desorption tests is urea formation [e.g. 10, 16, 36, 44]. The comparison between fresh VPOC1065 and A109 and the sample after cyclic tests are shown in Figs. 8a and 8b. The IR spectrum of both samples is reasonably similar as they are based on polystyrene divinylbenzene porous support. Both samples show considerable similarity with polystyrene FTIR spectrum.

For VPOC1065, bands at 698.36, 757.75, 817.14 cm^{-1} show C-H aromatic bending, 1377.6 and 1456.6 cm^{-1} show CH_2 bending, 1570.6 cm^{-1} show C=C aromatic ring bending. Alkyl C-H Stretching bands show at 2851.12 and 2918 cm^{-1}, 3029.4 cm^{-1} show C-H aromatic ring stretch and N-H amine stretching band shows at 3363.4 cm^{-1}.

About formation of carbamate or bicarbonate, Alesi and Kitchin [16] stated that $NCOO^-$ skeletal vibrations show at 1320, 1431, and 1482 cm^{-1} and $NCOO^-$ stretching band show at 1565cm^{-1}. Seems after desorption at 105^oC carbamate and bicarbonates are desorbed. For both A109 and VPOC1065 there is no considerable change between fresh samples and samples after adsorption-desorption cycles. There is stronger peak at about 2918 cm^{-1} for VPOC1065 that based on the work of sayari and Belmabkhout [10] belongs to urea formation.

A109 has a support similar to VPOC1065. Peaks in the region of 860 - 680 cm^{-1} generally show Aromatic C-H Bending. CH_2 bending of alkane shows at 1370.2 and 1450.8 cm^{-1}. Bands 1509.5 to 1681.8 cm^{-1} indicate Aromatic C=C Bending. Alkyl C-H Stretch bands show at 2854.6 and 2920.6 cm^{-1}. 3023.2 cm^{-1} belong to C-H aromatic ring stretch. There is stronger peak at about 2920.6 cm^{-1} that based on the work of sayari and Belmabkhout [10] belong to urea formation.

Both A109 and VPOC1065 show stronger adsorption at about 2920 cm^{-1} belong to urea formation. Urea is not removed by desorption in dry conditions. It seems that A109 shows stronger peak at 2920 cm^{-1} than VPOPC1065 indicating more urea formation and may be related to more capacity reduction of A109 in cyclic adsorption-desorption tests.

Conclusion

Five different ion exchange resins were studied in this work namely D201, D202, A830, A109 and VPOC1065. The adsorption performance of Purolite A109 and Lewatit VPOPC1065, which are functionalised with primary amines, were further investigated at different adsorption temperatures and CO_2/N_2 ratios. VPOC1065 shows higher adsorption capacity than A109 at all conditions due to the higher amine loading for VPOC1065 based on the manufacturer data sheet and CHN elemental analysis and possibly because of a different amine group.

Three different zones of CO_2 adsorption were distinguished by using CO_2 adsorption acceleration graphs. In the first zone, we have high rate of adsorption with positive CO_2 acceleration. The 2nd zone is a transition zone with negative acceleration. Third zone has low rate of adsorption with zero acceleration.

The results show that VPOC1065 displays an excellent stability after 275 cycles of adsorption-desorption with just 4.77% reduction in capture capacity.

With respect to rate of CO_2 adsorption and desorption, relatively mild desorption conditions and long term stability after 275 cyclic adsorption-desorption tests fort VPOC1065, it can be concluded that these resins are promising candidates for CO_2 capture. With respect to the theoretical capacity, ion exchange resins should be further optimised for CO_2 capture to obtain higher practical capture capacity.

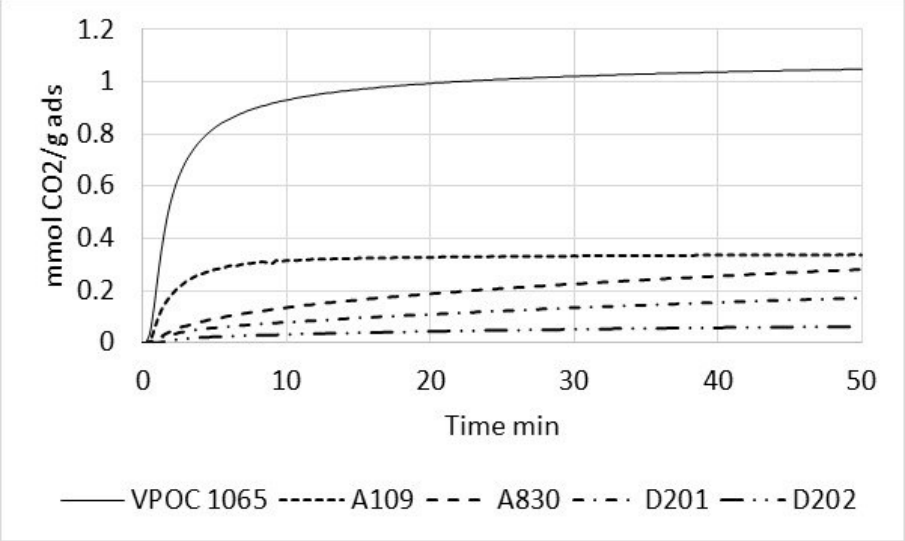

Fig. 1.

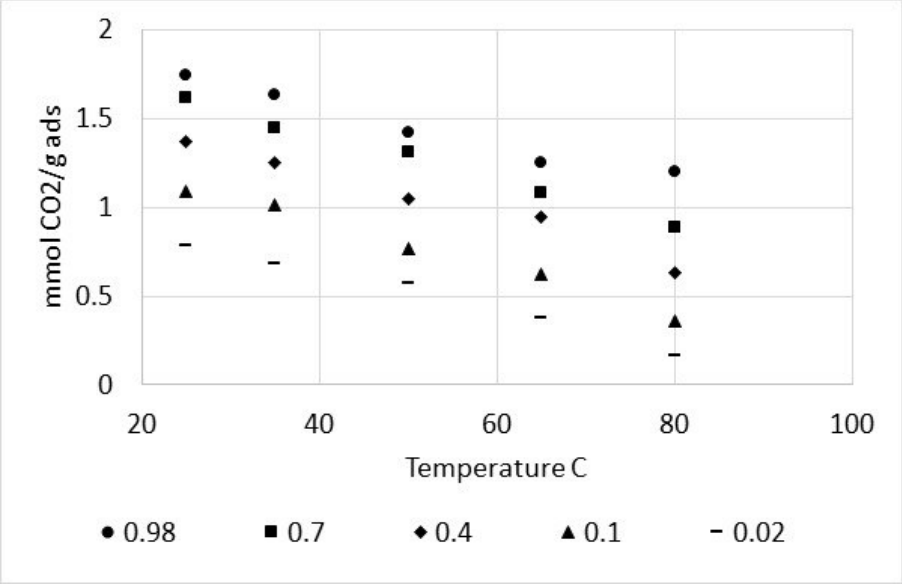

Fig. 2a.

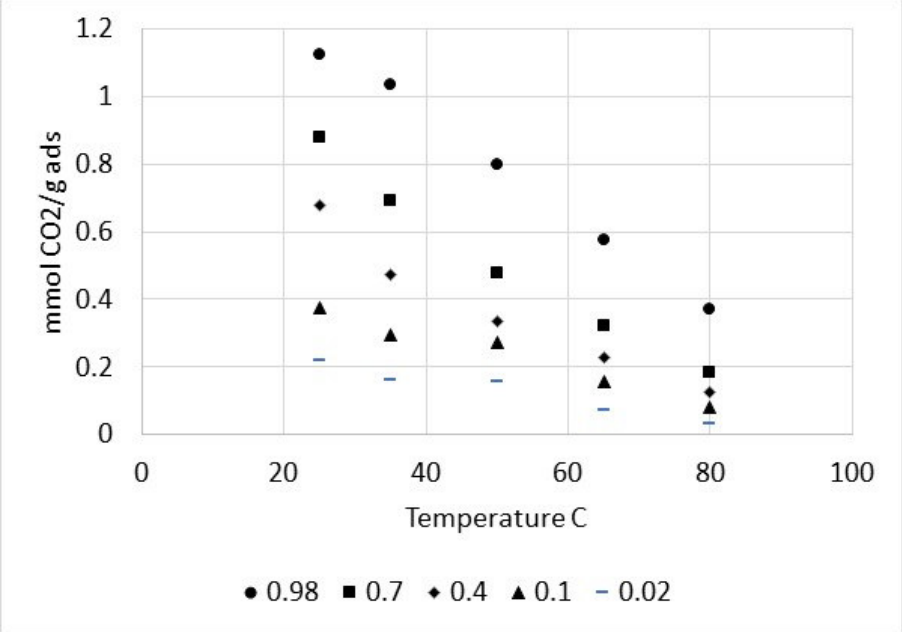

Fig. 2b.

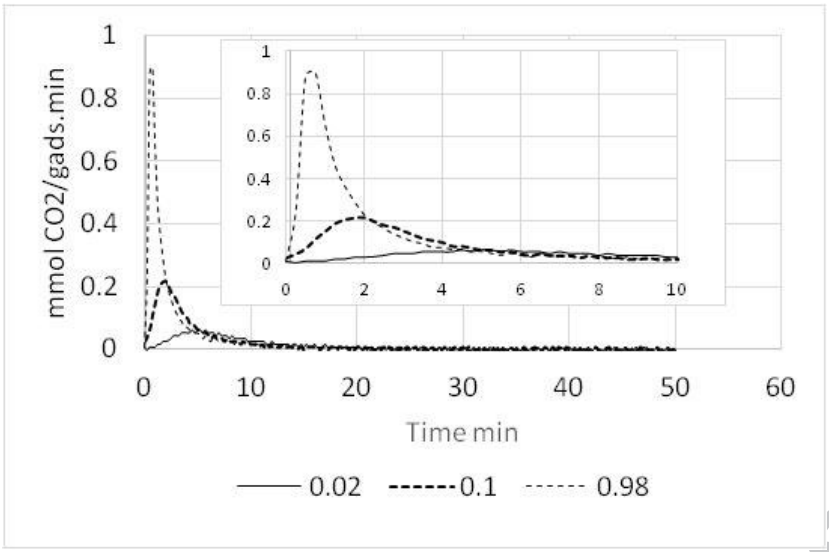

Fig. 3a.

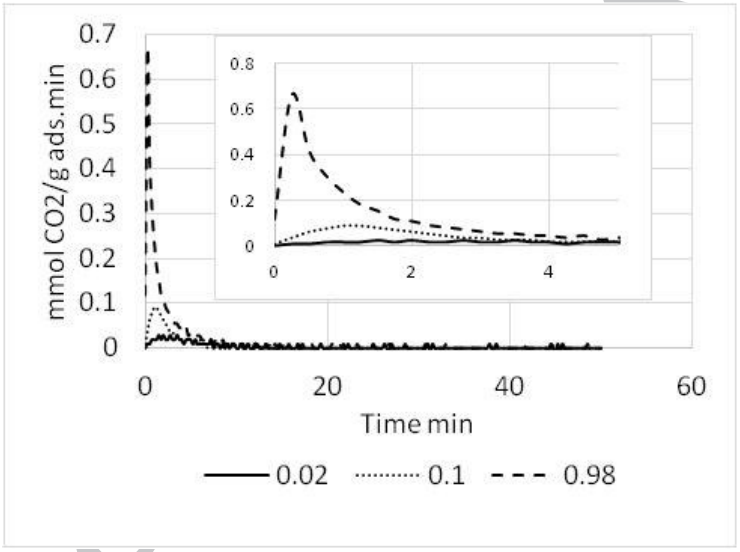

Fig. 3b.

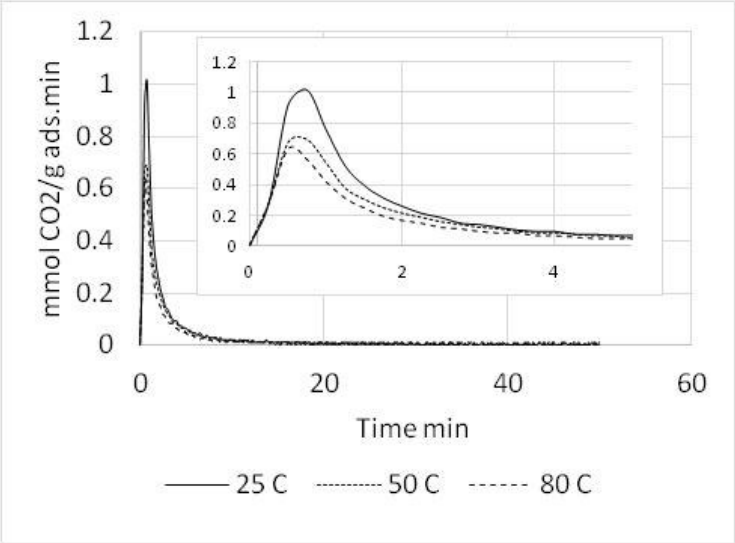

Fig. 4a.

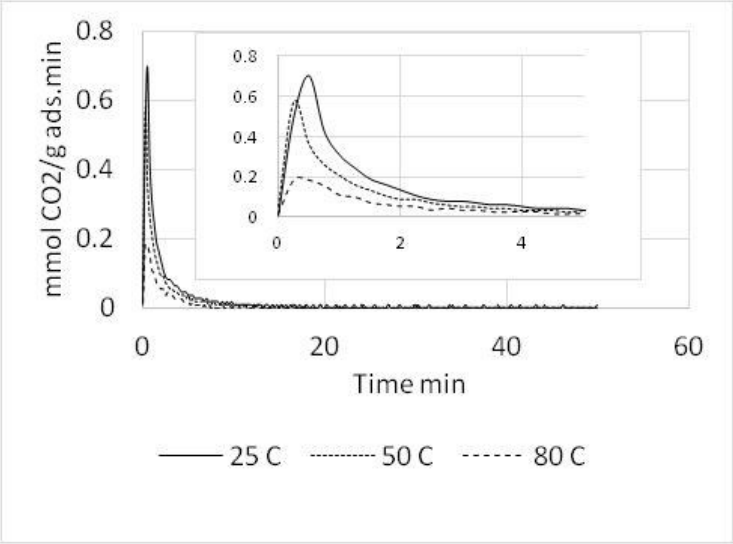

Fig. 4b.

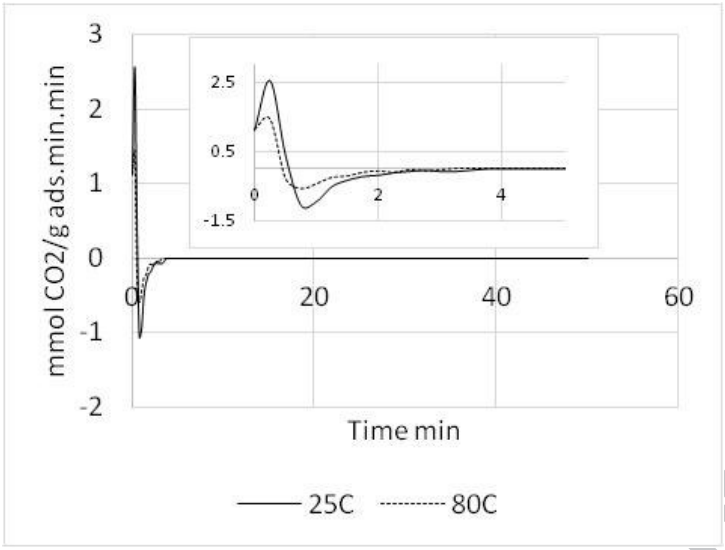

Fig. 5a.

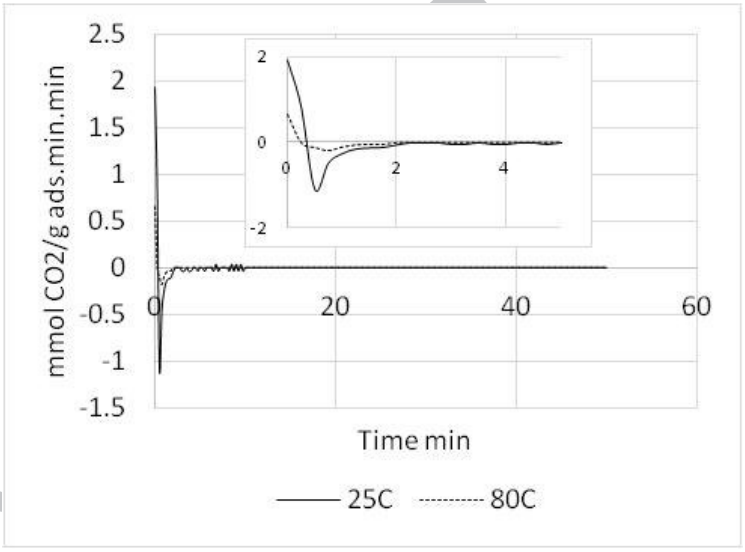

Fig. 5b.

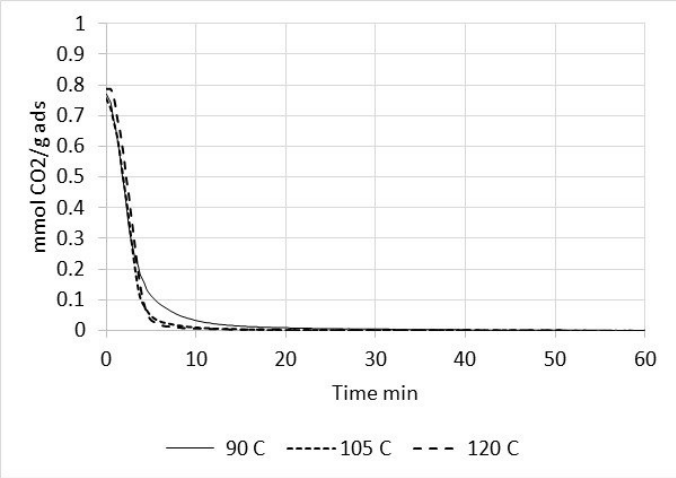

Fig. 6a.

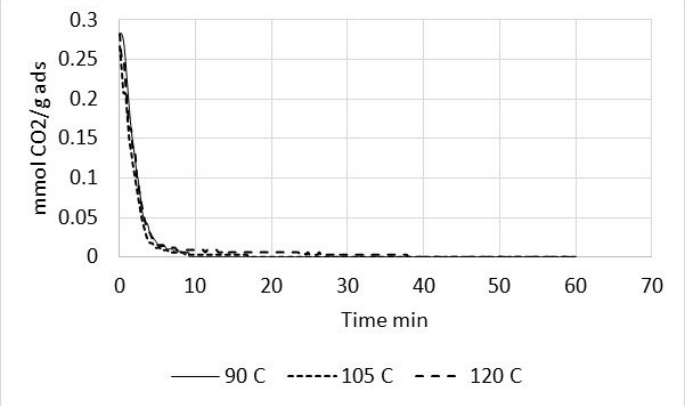

Fig. 6b.

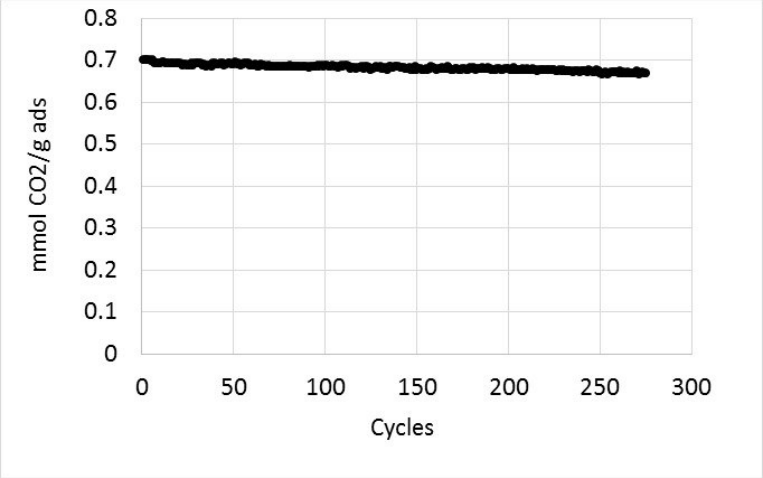

Fig. 7a.

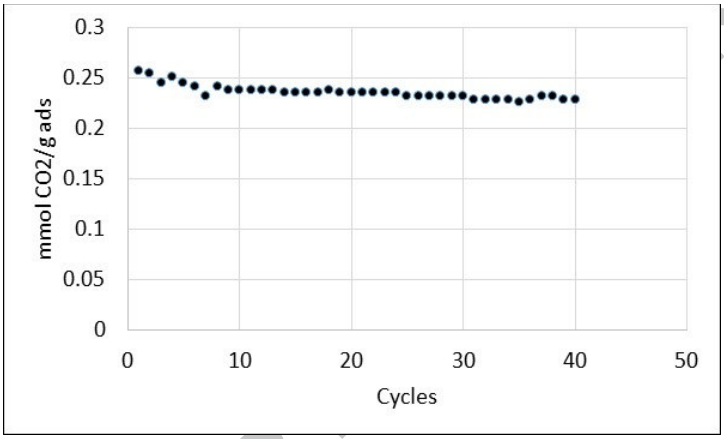

Fig. 7b.

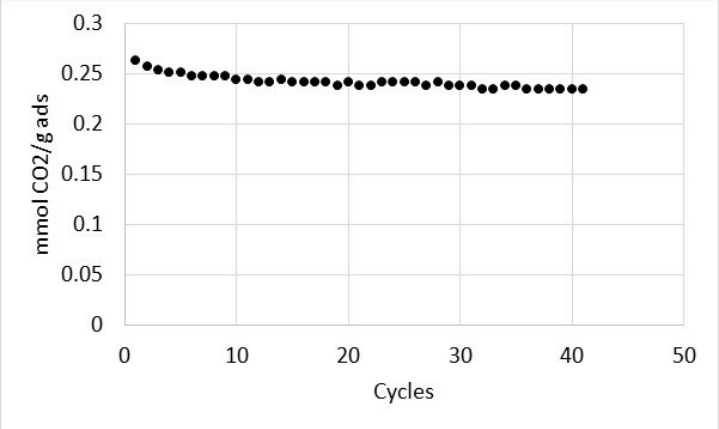

Fig. 7c.

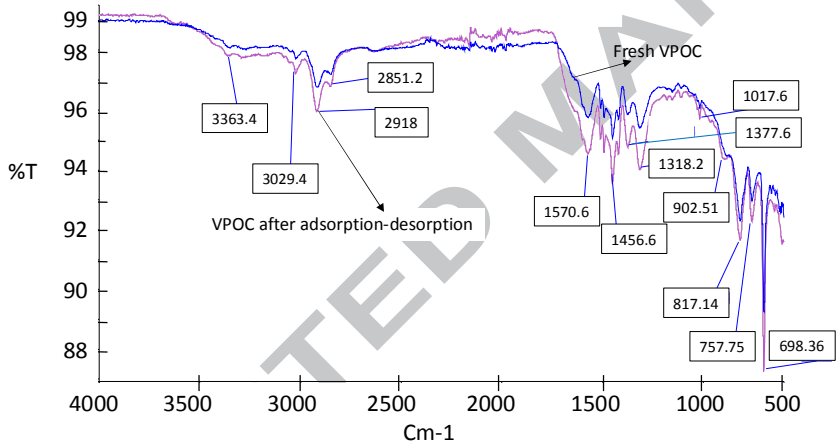

Fig. 8a.

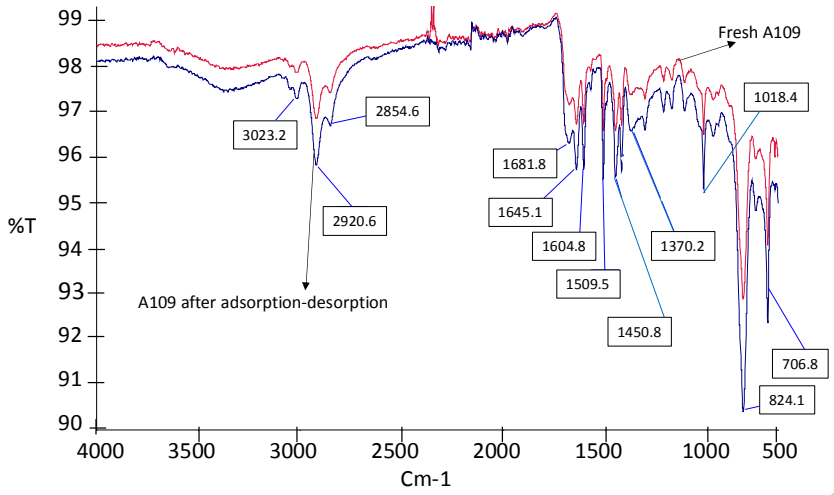

Fig. 8b.

List of Figures' Captions

Fig. 1. Comparison of CO_2 uptake by different commercial samples at 50°C and 0.4 CO_2/N_2.

Fig. 2a. CO_2 uptake by VPOC1065 at different temperatures and CO_2/N_2 ratio after 50 min of exposure to CO_2/N_2 gas mixture.

Fig. 2b. CO_2 uptake by A109 at different temperatures and CO_2/N_2 ratio after 50 min of exposure to CO_2/N_2 gas mixture.

Fig. 3a. Rate of CO_2 adsorption for VPOC1065 at different CO_2/N_2 ratio and 35°C.

Fig. 3b. Rate of CO_2 adsorption for A109 at different CO_2/N_2 ratio and 35°C.

Fig. 4a. Rate of CO_2 adsorption for VPOC1065 at different temperatures and 0.98 CO_2/N_2.

Fig. 4b. Rate of CO_2 adsorption for A109 at different temperatures and 0.98 CO_2/N_2.

Fig. 5a. CO_2 adsorption acceleration for VPOC1065 at 25 and 80°C and 0.98 CO_2/N_2.

Fig. 5b. CO_2 adsorption acceleration for A109 at 25 and 80°C and 0.98 CO_2/N_2.

Fig. 6a. CO_2 desorption for VPOC1065 at different desorption temperatures under pure N_2, CO_2 adsorption temperature of 50°C and 0.1 CO_2/N_2.

Fig. 6b. CO_2 desorption for A109 at different desorption temperatures under pure N_2, CO_2 adsorption temperature of 50°C and 0.1 CO_2/N_2.

Fig. 7a. Working capacity under 275 cycles of adsorption-desorption for VPOC1065, CO_2 adsorption at 50°C and 0.1 CO_2/N_2, desorption at 105°C with pure N_2.

Fig. 7b. Working capacity under 40 cycles of adsorption-desorption for A109, CO_2 adsorption at 50°C and 0.1 CO_2/N_2, desorption at 105°C with pure N_2.

Fig. 7c. Working capacity under 40 cycles of adsorption-desorption for A109, CO_2 adsorption at 50°C and 0.1 CO_2/N_2, desorption at 90°C with pure N_2.

Fig. 8a. FTIR spectra of VPOC1065 before and after cyclic adsorption-desorption tests.

Fig. 8b. FTIR spectra of A109 before and after cyclic adsorption-desorption tests.

References

1. B. Dutcher, M. Fan, A. G. Russell, Amine-Based CO2 Capture Technology Development from the beginning of 2013-A Review, Appl. Mater. Interfaces 7 **(**2015) 2137–2148.
2. X. Xu, C.S. Song, B.G. Miller, A.W. Scaroni, Adsorption separation of carbon dioxide from flue gas of natural gas-fired boiler by a novel nanoporous "molecular basket" adsorbent. Fuel Process. Technol. 86 (2005) 1457–1472.
3. S. Choi, J.H. Drese, C.W. Jones, Adsorbent materials for carbon dioxide capture from large anthropogenic point sources. Chem-SusChem 2 (2009) 796–854.
4. B. P. Spigarelli, S. K. Kawatra, Opportunities and challenges in carbon dioxide capture, J CO2 Util, 1 (2013) 69–87.
5. D. Aaron, C. Tsourism Separation of CO_2 from Flue Gas: A Review, Sep. Sci. Technol, 40 (2005) 321–348.
6. A. Sayari, Y. Belmabkhout, R. Serna-Guerrero, Flue Gas Treatment via CO2 Adsorption. *Chem. Eng. J.* 171 (2011) 760–774.
7. Y. Cheng-Hsiu, H. Chih-Hung, T. Chung-Sung Tan, A Review of CO2 Capture by Absorption and Adsorption, *Aerosol and Air Quality Res.* 12 (2012) 745–769.
8. Y, Zhao, L. Zhao, K. Xin Yao, Y. Yang, Q. Zhangc, Y. Han, Novel porous carbon materials with ultrahigh nitrogen contents for selective CO2 capture, J. Mater. Chem. 22 (2012) 19726–19731.
9. A. Samanta, A. Zhao, G. K. H. Shimizu, P. Sarkar, R. Gupta, Post-Combustion CO2 Capture Using Solid Sorbents: A Review, Ind. Eng. Chem. Res. 51 (2012), 1438–1463.
10. A. Sayari, Y. Belmabkhout, Stabilization of Amine-Containing CO2 Adsorbents: Dramatic Effect of Water Vapor, J. AM. CHEM. SOC. 132 (2010) 6312–6314.
11. Y.-C. Lee, S. M. Lee , W. G. Hong, Y. S. Huh, S. Y. Park, S. C. Lee, J. Lee, J. B. Lee, H. U. Lee, H. J. Kim, Carbon dioxide capture on primary amine groups entrapped in activated carbon at low temperatures, J. Ind. Eng. Chem. 23 (2015) 16–20.
12. W.-J. Son, J.-S. Choi, W.-S. Ahn, Adsorptive removal of carbon dioxide using polyethyleneimine-loaded mesoporous silica materials, Microporous and Mesoporous Mater. 113 (2008) 31–40
13. G. Qi, Y. Wang, L. Estevez, X. Duan, N. Anako, A.-H. A. Park,W. Li, C. W. Jones, E. P. Giannelis, High efficiency nanocomposite sorbents for CO2 capture based on amine-functionalized mesoporous capsules, Energy Environ. Sci. 4 (2011) 444–452.
14. C. Chen, W.-J. Son, K.-S. You, J.-W. Ahn, W.-S. Ahn, Carbon dioxide capture using amine-impregnated HMS having textural mesoporosity, Chem. Eng. J. 161 (2010) 46–52.
15. Y. Kuwahara, D.-Y. Kang, J. R. Copeland, P. Bollini, C. Sievers, T. Kamegawa, H. Yamashita, C. W. Jones, Enhanced CO2 adsorption over polymeric amines supported on heteroatom-incorporated SBA-15 silica: Impact of heteroatom type and loading on sorbent structure and adsorption performance, Chem. Eur. J. 18 (2012) 16649 – 16664.
16. W. R. Alesi Jr., J. R. Kitchin, Evaluation of a Primary Amine-Functionalized Ion-Exchange Resin for CO2 Capture, Ind. Eng. Chem. Res. 51 (2012), 6907−6915
17. O. Leal, C. Bolívar, C. Ovalles, J.J. García, Y. Espidel, Reversible Adsorption of Carbon Dioxide on Amine Surface-Bonded Silica Gel. *Inorg. Chim. Acta* 240 (1995) 183–189.
18. N. Hiyoshi, K. Yogo, T. Yashima, Adsorption Characteristics of Carbon Dioxide on Organically Functionalized SBA-15. Microporous Mesoporous Mater. 84 (2005) 357–365.
19. P. J. E. Harlick, A. Sayari, Applications of Pore-Expanded Mesoporous Silica. 5. Triamine Grafted Material with Exceptional CO2 Dynamic and Equilibrium Adsorption Performance, Ind. Eng. Chem. Res. 46 (2007), 446-458.
20. R. S. Guerrero, Y. Belmabkhoutb, A.Sayari, Further investigations of CO2 capture using triamine-grafted pore-expanded mesoporous silica, Chem. Eng. J. 158 (2010) 513–519.

21. Y. Jing , L. Wei, Y. Wang, Y. Yu, Synthesis, characterization and CO2 capture of mesoporous SBA-15 adsorbents functionalized with melamine-based and acrylate-based amine dendrimers, Microporous and Mesoporous Mater. 183 (2014) 124–133.
22. T. Filburn, J. J. Helble, R. A. Weiss, Development of Supported Ethanolamines and Modified Ethanolamines for CO2 Capture, Ind. Eng. Chem. Res. 44 (2005), 1542-1546
23. D. H. Jo, H. Jung, D. K. Shin, C. H. Lee, S. H. Kim, Effect of amine structure on CO2 adsorption over tetraethylenepentamine impregnated poly methyl methacrylate supports, Sep. Purif. Technol 125 (2014) 187–193.
24. M.L. Gray, K.J. Champagne, D. Fauth, J.P. Baltrus, Henry Pennline, Performance of immobilized tertiary amine solid sorbents for the capture of carbon dioxide, Int. j. greenhouse gas control 2 (2 0 0 8) 3 – 8.
25. M. L. Gray, J. S. Hoffman, D. C. Hreha, D. J. Fauth, S. W. Hedges, K. J. Champagne,H. W. Pennline, Parametric Study of Solid Amine Sorbents for the Capture of Carbon Dioxide Energ. Fuel. 23 (2009) 4840–4844.
26. R. Veneman, Z.S. Li, J.A. Hogendoorn, S.R.A. Kersten , D.W.F. Brilman, Continuous CO2 capture in a circulating fluidized bed using supported amine Sorbents, Chem. Eng J 207–208 (2012) 18–26.
27. J. Wang, M. Wang, W. Li, W. Qiao, D. Long, L. Ling, Application of Polyethylenimine-Impregnated Solid Adsorbents for Direct Capture of Low-Concentration CO2, AIChE J. 61 (2015) 972-980.
28. C. F. Martin, E. Stockel, R. Clowes, D. J. Adams, A. I. Cooper, J. J. Pis, F. Rubiera, C. Pevida, Hypercrosslinked organic polymer networks as potential adsorbents for pre-combustion CO2 capture, J. Mater. Chem. 21 (2011) 5475–5483.
29. R. Gomes, A. Bhaumik, Highly porous organic polymers bearing tertiary amine group and their exceptionally high CO2 uptake capacities, J. Solid State Chem. 222 (2015) 7–11.
30. H. He,W. Li, M. Lamson, M. Zhong, D. Konkolewicz, C. M. Hui, K. Yaccato, T. Rappold, G. Sugar, N.E. David, K. Damodaran , S. Natesakhawat, H. Nulwala, K. Matyjaszewski, Porous polymers prepared via high internal phase emulsion polymerization for reversible CO2 capture, Polymer 55 (2014) 385-394.
31. S. Makhseed, J. Samuel, Imide-linked microporous organic framework polymers for CO2 adsorption, Polymer 74 (2015) 144-149.
32. N. Manoranjan, D. H. Won, J. Kimb, S. I. Woo, Amide linked conjugated porous polymers for effective CO2 capture and separation, Journal of CO2 Utilization 16 (2016) 486-491.
33. M. G. Rabbani, H. M. El-Kaderi, Synthesis and Characterization of Porous Benzimidazole-Linked Polymers and Their Performance in Small Gas Storage and Selective Uptake, Chem. Mater. 24 (2012) 1511−1517.
34. M. Saleh, S. B. Baek, H. M. Lee, K. S. Kim, Triazine-Based Microporous Polymers for Selective Adsorption of CO2, J. Phys. Chem. C 119 (2015) 5395−5402.
35. T. Chitsiga, M. O. Daramola, N. Wagner, J. Ngoy, Effect of the presence of water-soluble amines on the carbon dioxide (CO2) adsorption capacity of amine-grafted polysuccinimide (PSI) adsorbent during CO2 capture, Energy Procedia 86 (2016) 90 – 105.
36. R. Veneman, N. Frigka, W. Zhao, Z. Li, S. Kersten, W. Brilman, Adsorption of H_2O and CO_2 on supported amine sorbents, Int. J. Greenhouse Gas Control 41 (2015) 268–275.
37. A.P. Hallenbeck, J. R. Kitchin, Effects of O2 and SO2 on the Capture Capacity of a Primary-Amine Based Polymeric CO2 Sorbent Ind. Eng. Chem. Res. 52 (2013) 10788−10794.
38. S. Kim, J. Ida, V. V. Guliants, J. Y. S. Lin, Tailoring Pore Properties of MCM-48 Silica for Selective Adsorption of CO2, J. Phys. Chem. B 109 (2005) 6287-6293.
39. M.B. Yue, L. B. Sun, Y. Cao, Y. Wang, Z. J. Wang, J. H. Zhu, Efficient CO2 Capturer Derived from As-Synthesized MCM-41 Modified with Amine, Chem. Eur. J. 14 (2008) 3442 – 3451.
40. V. Zelenak , D. Halamova , L. Gaberova , E. Bloch, P. Llewellyn, Amine-modified SBA-12 mesoporous silica for carbon dioxide capture: Effect of amine basicity on sorption properties, Microporous and Mesoporous Mater. 116 (2008) 358–364.
41. R. Sanz, G. Calleja , A. Arencibia, E. S. Sanz-Pérez, Amino functionalized mesostructured SBA-15 silica for CO2 capture: Exploring the relation between the adsorption capacity and the distribution of amino groups by TEM, Microporous and Mesoporous Mater. 158 (2012) 309–317.
42. T. Chitsiga, M. O. Daramola, N. Wagner, J. Ngoy, Effect of the presence of water-soluble amines on the carbon dioxide (CO2) adsorption capacity of amine-grafted polysuccinimide (PSI) adsorbent during CO2 capture, Energy Procedia 86 (2016) 90 – 105.

43. S. Meth, A. Goeppert, G. K. S. Prakash, G. A. Olah, Silica Nanoparticles as Supports for Regenerable CO2 Sorbents, Energ. Fuel. 26 (2012) 3082−3090.
44. K. Li , J.O Jiang , F. Yan , S. Tian , X. Chen, The influence of polyethyleneimine type and molecular weight on the CO2 capture performance of PEI-nano silica adsorbents, Appl. Energ. 136 (2014) 750–755.

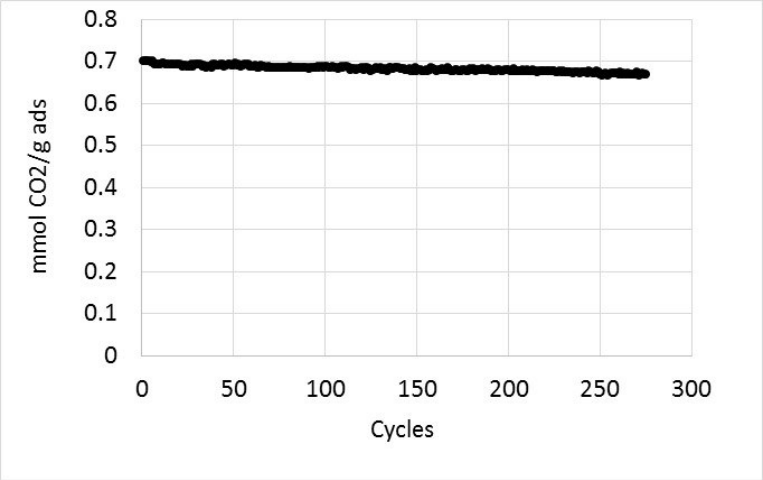

ACCEPTED MANUSCRIPT

- ○○○Distinguishing adsorption zones by using adsorption acceleration graphs
- Excellent cyclic adsorption-desorption stability after 275 cycles for VPOC1065
- Fast and complete CO_2 desorption at 105^{o}C based on desorption graphs and IR absorption data for both A109 and VPOC1065